Macromolecules
ARTICLE

Macromolecules **2009**, *42*, 5461–5470 **5461**
DOI: 10.1021/ma900905k

Cytoskeleton Mimetic Reinforcement of a Self-Assembled *N,N′*-Dialkylimidazolium Ionic Liquid Monomer by Copolymerization

Simonida Grubjesic,[†] Sönke Seifert,[‡] and Millicent A. Firestone*,[†]

[†]*Materials Science and* [‡]*X-ray Sciences Divisions, Argonne National Laboratory, 9700 South Cass Avenue, Argonne, Illinois 60439*

Received April 25, 2009; Revised Manuscript Received April 30, 2009

ABSTRACT: Preparation and photopolymerization of a decylmethylimidazolium ionic liquid (IL) that possesses an acrylate counteranion are described. This IL monomer self-assembles upon addition of water and can be copolymerized with poly(ethylene glycol) diacrylate (PEGDA) in the presence of a photoinitiator, forming a mechanically durable material that adopts a lamellar structure with in-plane hexagonally ordered pores, as evidenced by small-angle X-ray scattering (SAXS). Thermogravimetric analysis, the extent of polymerization, and solubility−swelling studies indicate the formation of a network copolymer of the IL monomer and the PEGDA. Additional evidence for the formation of a nanostructured copolymer is provided by evaluating the product formed by replacement of the IL monomer with the nonpolymerizable analogue, decylmethylimidazolium chloride. The results demonstrate the possibility of designing a self-assembled amiphiphilic bilayer architecture that is reinforced by polymerization and cross-linking.

Introduction

In nature, cell membranes are stabilized by structural biopolymers, cytoskeletons that consist of a flat, hydrophilic protein network at the membrane surface linked by anchor proteins to the membrane.[1] Although considerable work has been devoted to the preparation and evaluation of amiphiphilic bilayer structures as biomembrane mimics, less effort has been directed at the preparation of self-assembled materials that more fully mimic the complexity of natural cell membranes.[2] For example, self-assembled architectures are needed that incorporate a structural scaffold that improves the mechanical stability of the membrane while not impeding the insertion or association of membrane proteins. The future development of protein-based materials (and ultimately devices) requires that the native functionality of membrane proteins be preserved and exploited. Accordingly, it is important to develop artificial systems that can mechanically stabilize amphiphilic bilayer architectures (i.e., cytoskeleton mimics). Several strategies for using synthetic polymers as cytoskeleton mimics, including surface coating with oppositely charged polyelectrolytes[3−5] or hydrophobically anchoring polymers[6−8] to vesicles or liposomes, have been described previously.[9] These approaches can, however, cause undesirable vesicle fusion or disruption of the bilayer structure. An alternative approach involves the polymerization of the self-assembled amiphiphiles themselves.[10,11] This strategy can afford greater stability but impedes membrane solute insertion or transbilayer transport and restricts the lateral mobility of the amiphiphiles (i.e., lipids). An alternative that has not been fully explored is the cross-linking polymerization of monomers that are associated (i.e., electrostatically, hydrophobic membrane insertion) with the organized amphiphiles.[12,13]

We have demonstrated previously that the introduction of polymerizable moieties on a *N*-dialkylimidazolium cation (i.e., 1-decyl-3-methylimidazolium, [C_{10}mim$^+$]) can yield ionic liquid monomers that self-assemble into well-ordered mesophases when dispersed in water.[14−16] Replacement of the methyl group with a vinyl moiety to give a 1-decyl-3-vinylimidazolium chloride salt (i.e., [C_{10}Vim$^+$][Cl$^-$]), for example, permitted polymerization at the cation headgroup.[14] Similar results were obtained by appending an acryloyl group on the terminus of the alkyl chain to yield, for example, (1-(8-(acryloyloxy)octyl)-3-methylimidazolium chloride, [AcrC_8mim$^+$][Cl$^-$]. [15] In both instances UV photopolymerization of the self-assembled binary mixtures yielded self-supporting, durable chemical gels. These polymers were shown to be reversibly swollen in a range of solvents; thus, they could serve as dynamic nanostructures.[14,15] It was further demonstrated that metal nanoparticles could be readily synthesized during this UV-initiated polymerization.[14] Although these IL-derived polymers were shown to be versatile soft nanostructures, they are plagued by a significant limitation, namely, the inaccessibiliy of the bilayer to membrane proteins. Specifically, the position of the polymerizable moieties on either the cation headgroup or the alkyl chain terminus inhibits insertion of membrane-soluble biomolecules. To produce a material more amenable to membrane protein stabilization (that is, one that would leave the bilayer architecture intact), we examine here the possibility of IL polymerization/cross-linking through the *counteranion*. Specifically, we describe the preparation of 1-decyl-3-methylimidazolium acrylate, ([C_{10}mim$^+$][Acr$^-$]), an IL monomer that incorporates a polymerizable anion, examine its self-assembly in water, and study its thermal properties and isothermal swelling in a variety of solvents. Photopolymerization of the self-assembled monomeric amphiphile with the addition of a comonomer, poly(ethylene glycol) diacrylate (PEGDA), a common biocompatible, water-soluble cross-linking monomer,[17,18] is described and characterized.

Experimental Section

Materials and Methods. 1-Decyl-3-methylimidazolium halides, [C_{10}mim$^+$][Br$^-$] and [C_{10}mim$^+$][Cl$^-$], were purchased from EMD Chemicals (Gibbstown, NJ). Silver acrylate was

*To whom correspondence should be addressed: Ph 630-252-8298; Fax 630-252-9151; e-mail firestone@anl.gov.

Published on Web 05/21/2009

purchased from Gelest (Morrisville, PA). Darocur 1173 was received as a gift from Ciba Chemicals (Tarrytown, NY). All other chemicals were purchased and used as received from Sigma-Aldrich (Milwaukee, WI). Water used in all experiments was of nanopure quality, 18 MΩ.

Monomer and Copolymer Synthesis. *1-Decyl-3-methylimidazolium Acrylate, [$C_{10}mim^+$][CH_2=$CHCOO^-$], [C10mim$^+$][Acr$^-$] (**1**).* Silver acrylate (267 mg, 1.49 mmol) was added to a solution of [$C_{10}mim^+$][Br^-] (508.3 mg, 1.67 mmol) in water (5 mL) and stirred for 3 days at 21 °C under an argon atmosphere. The reaction mixture was filtered through 0.45 μm syringe filter and freeze-dried. The resulting pale yellow liquid (445 mg, 99%). ^{1}H NMR (500 MHz, $CDCl_3$) δ (ppm): 10.65 (s, 1H), 7.29 (d, J = 1.9, 1H), 7.19 (d, J = 1.9, 1H), 6.19 (dd, J = 17.3, 10.1, 1H), 6.00 (dd, J = 17.3, 2.5 1H), 5.36 (dd, J = 10.1, 2.5, 1H), 4.23 (t, J = 7.4, 2H), 4.02 (s, 3H), 1.82 (t, J = 7.0, 2H), 1.27 (t, J = 7.4, 2H), 1.22 (m, 12H), 0.85 (t, J = 7.4, 3H). ^{13}C NMR (500 MHz, CD_3CN) δ (ppm): 172.9, 137.6, 122.9, 122.5, 121.1, 49.8, 36.3, 31.8, 30.2, 29.4, 29.3, 29.2, 29.0, 26.2, 22.6, 14.1. Anal. Calcd for $C_{17}H_{30}N_2O_2$: with adjustment for water content and presence of [$C_{10}mim^+$][Br^-]: C, 61.14; H, 10.22, N, 8.53. Found: C, 61.54; H, 10.08; N, 8.60. Stable storage of the monomer can be achieved in the dark at 4 °C.

Net-poly(1-decyl-3-methylimidazolium acrylate)-co-poly(ethylene glycol) diacrylate, Net-*poly[$C_{10}mim^+$][Acr^-]-co-PEGDA*. In a $^1/_2$ dram vial, water (2 μL) was added to 1-decyl-3-methylimidazolium acrylate (31.3 mg, 0.095 mmol). (The initial water content of the starting monomer was 10% w/w as measured by TGA, making the total calculated aqueous content 8% w/w.) The tightly capped vial was heated at ∼60 °C and vortex mixed until a homogeneous mixture was obtained. Poly(ethylene glycol) diacrylate (M_n 575, MW 508, 24 μL, ca. 0.048 mmol) was added to the reaction mixture and vortex mixed followed by the addition of Darocur 1173 (0.5 μL). The reaction mixture was vortex mixed and heated to ∼60 °C for 5 min prior to loading a portion of the hot mixture into borosilicate glass pipet (∼2−3 in.) using negative pressure. The pipet was allowed to cool to RT and clipped from its wider end. The sample was placed ∼6 in. away from a high-intensity UV light source (Hanovia 400 W mercury arc lamp, λ = 254 nm) and irradiated for 30 min. The resulting polymer was removed from the pipet by breaking the pipet glass with a razor blade.

Ionic Liquid Encapsulated in PEGDA. *1-Decyl-3-methylimidazolium Chloride, [$C_{10}mim^+$][Cl^-] Encapsulated in Net-poly (ethylene glycol) Diacrylate*. In a $^1/_2$ dram vial, water (24 μL) was added to 1-decyl-3-methylimidazolium chloride (100.0 mg, 0.39 mmol). (The initial water content of the starting ionic liquid was 5% w/w as measured by TGA, making the total calculated aqueous content 12% w/w.) The tightly capped vial was heated at ∼60 °C and vortex mixed until a homogeneous mixture was obtained. Poly(ethylene glycol) diacrylate (100 μL, ca. 1.9 mmol) was added to reaction mixture and vortex mixed followed by the addition of Darocur 1173 (2 μL). The reaction mixture was vortex mixed and heated at ∼60 °C for 5 min prior to loading a portion of the hot mixture into borosilicate glass pipet (∼2−3 in.) using negative pressure. The pipet was allowed to cool to RT and clipped from its wider end. The sample was placed ∼6 in. away from a high-intensity UV light source (Hanovia 400 W mercury arc lamp, λ = 254 nm) and irradiated for 30 min. The resulting polymer was removed from the pipet by breaking the pipet glass with a razor blade.

Extent of Polymerization. The extent of monomer to polymer conversion was determined by ^{1}H NMR.[19] Briefly, a photopolymerized material of known weight was Soxhlet extracted in ethanol to reclaim any residual, unreacted monomer. The ethanol was taken to dryness by rotary evaporation, and the remaining residue solubilized in MeCN-d_3 (1 mL). The sample was spiked with a ferrocene standard (7.5 mg, 40 μmol) and transferred to a 5 mm NMR tube. The ratio of the number of protons from the monomer (as indicated by the amount of aromatic protons) to ferrocene (δ 4.1 ppm) in the ^{1}H NMR spectrum (using spectrometer integration values) was used to estimate the number of moles of recovered monomer or ionic liquid.

Physical Methods. Differential scanning calorimetry (DSC) was performed on a Q100 instrument (TA Instruments, New Castle, DE) interfaced with a refrigerated cooling system. Weighed amounts (1−5 mg) of the sample were sealed in aluminum pans, and data were collected in the −75 to 150 °C range at a heating rate of 2 °C/min. Instrument calibration was performed using an indium standard. Thermogravimetric analysis (TGA) was carried out on a TA Instruments Q50 by heating a known amount of sample (1−5 mg) in a platinum pan from 20 °C to a final temperature of 500 °C at a rate of 10 °C/min under N_2 flow. Differential thermogravimetric (DTG) plots were derived from TG scans using the software supplied by the TA Instruments, and the temperature at the maximum rate of mass loss (peak in DTG) was recorded. All NMR experiments were performed on a Bruker model DMX 500 NMR spectrometer (11.7 T) equipped with a three-channel, 5 mm inverse detection, three-axis-gradient, variable-temperature probe with ^{2}H lock at 76.773 MHz. With the use of the nitrogen precooler, heater coil, and the variable temperature controller, the temperature was maintained at 295 K. Elemental analysis was performed by Galbraith Laboratories (Knoxville, TN). Polarized optical microscopy was performed on Baush & Lomb Micro Zoom microscope equipped with a custom-made Peltier temperature controller unit.

Small-angle X-ray scattering (SAXS) measurements were made using the instrument at undulator beamline 12ID-C,18ID or at the bending magnet beamline 12BM (11−12 keV) of the Advanced Photon Source at Argonne National Laboratory. The 2D scattering profiles were recorded with a MAR-CCD-165 detector (Mar USA, Evanston, IL), which features a circular, 165 mm diameter active area and 2048 × 2048 pixel resolution. The sample-to-detector distance was such as to provide a detecting range for momentum transfer of 0.001 Å^{-1} < q < 0.6 Å^{-1}. The scattering vector, q, was calibrated using a silver behenate standard at q = 1.076 Å^{-1}. The 2D scattering images were first corrected for spatial distortion and sensitivity of the detector and then radially averaged to produce plots of scattered intensity, $I(q)$, vs scattering vector, q, where is $q = 4\pi/\lambda(\sin\theta)$. The value of q is proportional to the inverse of the length scale, Å^{-1}. For these measurements, samples were probed either as freely suspended polymers or as the gels confined in glass capillaries. Measurements were made at 25 ± 1 °C.

Equilbrium Swelling in Various Solvents. Freshly synthesized *net*-poly[$C_{10}mim^+$][Acr^-]-*co*-PEGDA or [$C_{10}mim^+$][Cl^-] encapsulated in PEGDA composites were cut into cylindrical pieces with the dimensions 8.0−12.0 mm × 1.0 mm (L × W). Each piece was then fully immersed into one of the following solvents: hexanes, ethyl acetate (EtOAc), chloroform ($CHCl_3$), acetonitrile (ACN), dimethylformamide (DMF), ethanol, dimethyl sulfoxide (DMSO), and water. After 24 h, the samples were removed from the solvent and placed on a paper towel to remove excess solvent, and their length and width were measured. The volume of the sample was calculated, and a ratio of the volume (V) vs the initial volume (V_0) of the sample was determined (V/V_0). All measurements were made under ambient laboratory conditions: 21 °C (±1 °C), 53% (±3%) relative humidity.

Results and Discussion

An ionic liquid possessing a polymerizable anion, acrylate, was synthesized by a metathesis reaction involving the treatment of an aqueous solution of [$C_{10}mim^+$][Br^-] with silver acrylate. The accumulated solids (AgBr) were removed by filtration and the IL recovered (Scheme 1). The [$C_{10}mim^+$][Acr^-] (**1**) was confirmed by ^{1}H NMR spectroscopy and elemental analysis. The purified product was a very pale yellow, viscous liquid at room temperature.

Scheme 1. Synthesis of [C_{10}mim$^+$][Acr$^-$] Ionic Liquid Monomer

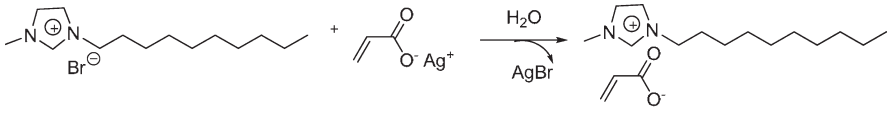

(1)

Monomer Thermal Properties. The DSC heating/cooling scan collected on a dried monomer **1** over the range −65 to 95 °C show several endo- and exothermic phase transitions (Figure 1A). Specifically, the heating profile on the monomer shows an endothermic peak at −37.6 °C which is assigned to the melting point, T_m, in agreement with the observed liquid appearance of the sample at room temperature. The T_m below 25 °C allows this IL monomer to be classified as a room temperature ionic liquid. The low melting point of [C_{10}mim$^+$][Acr$^-$] versus analogous inorganic C_{10}mim$^+$ salts (e.g., Cl$^-$ with T_m = 20.53 °C) is consistent with the established trend that ILs possessing organic anions typically have lower melting points.[20] Furthermore, the reduced T_m observed here may be due to multiple factors, including an increase in the anion size and a reduction in symmetry, which serves to both lower the packing efficiency and weaken intermolecular interactions (i.e., hydrogen bonding).[21] Addition of water to the dried IL, to yield a water content of 11% (w/w), causes the T_m to shift to −13.7 °C (Figure 1A, inset). The increase in the T_m compared to that found for the dried monomer most likely arises from water-induced changes in intermolecular interactions (i.e., water-mediated hydrogen bonding between cation and anion). It is noted that in addition to the melting point an endothermic transition occurs at 52.5 °C (Figure 1A, inset), which signals the transition from the liquid-crystalline to isotropic state as evidenced by the loss of the hexatic textures under polarized light. Additional information regarding the thermal properties of the IL monomer was obtained by fast scan (10 °C/min) thermogravimetric analysis (TGA) under a nitrogen atmosphere. Specifically the monomer shows a single-step decomposition profile at 244 °C (Figure 1B). This decomposition behavior compares well with that previously determined for both the [AcrC_8mim$^+$][Cl$^-$] and [C_{10}Vim$^+$][Cl$^-$].[14−16]

Similar to other amphiphilic IL monomers,[14,15] the [C_{10}mim$^+$][Acr$^-$] could be self-assembled when dispersed in water. Here this was achieved by the addition of water to yield a total content of 9 ± 2% (w/w). The binary mixture was a transparent, homogeneous, slightly viscous liquid (weak gel). At this water content a highly ordered liquid crystalline phase is produced as evidence by the strong optical birefringence observed when examined under polarized light (Figure 2A). The focal conic textures are suggestive of a columnar hexatic liquid-crystalline phase.[22] Addition of the comonomer (PEGDA, M_n 575, MW 508) and photoinitiator (Darocur 1173) to the lyotropic liquid crystal (i.e., the unpolymerized composition) yields a mixture showing very similar textures under polarized light (Figure 2A, inset). The retention of the liquid-crystalline textures upon addition of the additional water-soluble components (i.e., PEGDA and Darocur) indicate that they do not significantly impact the self-assembly of the IL monomer−water mixture.

Additional details regarding the mesoscopic structure of the unpolymerized (prior to UV irradiation) mixture of IL monomer, [C_{10}mim$^+$][Acr$^-$], and comonomer, PEGDA, dispersed in 11% (w/w) water containing a small amount of the photoinitiator was obtained by small-angle X-ray scattering (SAXS). The 2-D spot pattern shows six intense (10) reflections with 6-fold symmetry (Figure 2B). Such a pattern is characteristic of a 2-D hexagonal lattice in which the hexagonal cylinders are arranged primarily coincident with the incident X-rays.[22] These results differ from those observed for a randomly oriented liquid-crystalline material which would exhibit a circular, isotropic 2-D diffraction pattern. The relatively well-resolved Bragg diffraction spots indicate that the mixture consists primarily of large, hexagonal domains over the sample volume (ca. 50 μm^2) interrogated by the X-ray beam. The circularly averaged SAXS data (Figure 2C) show the presence of four well-resolved diffraction peaks at 1:$\sqrt{3}$:2:$\sqrt{7}$ (q = 0.233, 0.400, 0.458, 0.616 Å^{-1}), which further confirm a 2-D hexagonal lattice. The position of the first-order peak can be used to determine a lattice parameter $a = (2/\sqrt{3})d_{100}$ = 31.2 Å based upon the d_{100} = 27.0 Å. The observed assembly of the IL monomer/comonomer mixture into a hexagonal columnar mesophase is consistent with our prior observations that this architecture is favored for the methyldecylimidazolium halide ionic liquids.[14,16,22] More importantly, we find that the anion exchange of the halide for the larger, organic anion (acrylate) does not significantly impact the self-assembled structure.

Photopolymerization of the self-assembled mixture was achieved by UV irradiation at 254 nm for 30 min to yield a durable, self-supporting, glassy-like material (Figure 2D). Under polarized light, the cylindrical rod-shaped polymers were found to be highly birefringent (Figure 2D, inset). It is noted that all attempts to polymerize monomer **1** without the use of the comonomer, or employing other initiators (e.g., potassium persulfate and 2,2′-azobis(2-diisobutyramidine) dihydrochloride (AIBA)), using both thermal and photopolymerization did not yield durable, self-supporting materials. The extent of copolymerization was determined by extensive Soxhlet extraction of a known amount of material in ethanol. The ethanolic extract was collected and reduced under vacuum, and the residue redissolved in MeCN-d_3. The amount of the extracted [C_{10}mim$^+$][Acr$^-$] was then determined by ^{1}H spectroscopy by monitoring either the C-2 proton on the imidazolium cation[15] or the aromatic protons. The composition and polymerization conditions used here were found to yield a high percentage of IL monomer to polymer conversion (93 ± 4%).

The SAXS data collected on the photoirradiated product are shown in Figure 2E,F. The 2-D SAXS pattern (Figure 2E) shows an anisotropic pattern with the scattered X-ray intensity predominantly directed in the equatorial direction. The averaged data presented in Figure 2F possess a strong reflection at q = 0.219 Å^{-1} which contains two weak shoulders on either side of this peak at q = 0.200 and 0.253 Å^{-1}. These features positioned at 0.91q, q, 1.15q Å^{-1} index to the (101), (003), and (102) reflections of a hexagonal perforated lamellar (HPL) structure (Figure 3A). The HPL phase is believed to form in two steps, in which first random perforations within the lamellar sheets occur, giving rise to the low-q diffuse scattering.[23] In the second step, in-plane ordering of the perforations into a close-packed hexagonal array is accompanied by a reduction in the low-q scattering and evolution of the Bragg peaks toward those that index to a hexagonal lattice. Here, it is noted that a higher ordered (broad) reflection is observed at q = 0.366 Å^{-1} ($\sqrt{3}q$),

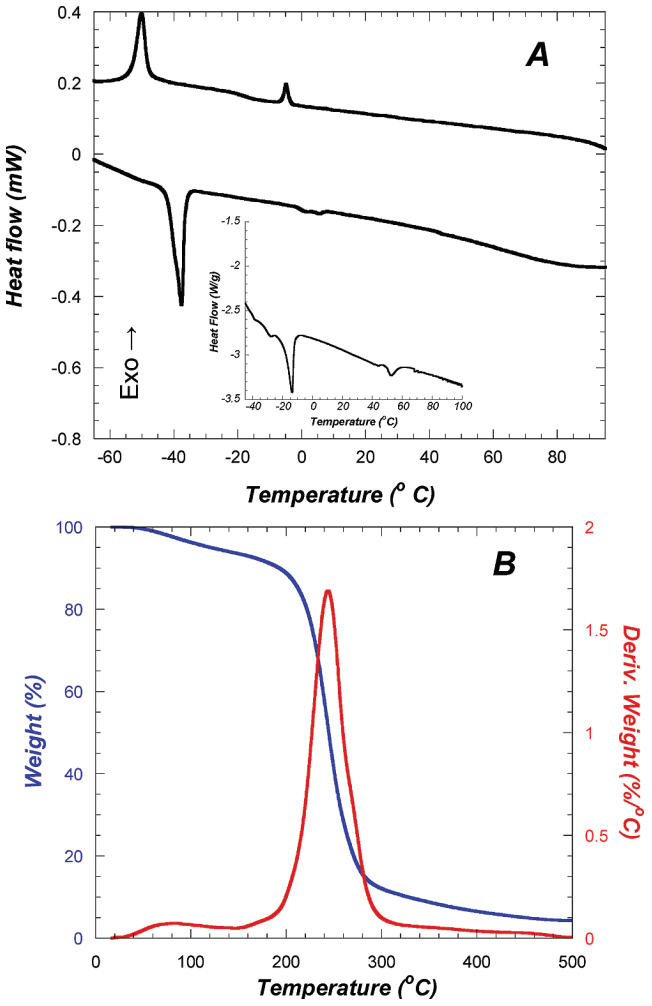

Figure 1. (A) DSC heating and cooling scans (2 °C/min) collected on dried, solid [C_{10}mim$^+$][Acr$^-$]. Inset shows a representative DSC heating scan (2 °C/min) collected on a binary mixture of 11% (w/w) water and [C_{10}mim$^+$][Acr$^-$]. (B) Fast scan (10 °C/min) TGA collected on [C_{10}mim$^+$][AC$^-$] under a N_2 atmosphere: weight % (blue) and derivative weight loss, DTG (red).

suggesting near complete formation of a close-packed arrangement of the pore structure (Figure 2F). The reduction of symmetry upon UV-induced polymerization has been observed previously for poly(vinyldecylimidazolium chloride) and was attributed to changes in the polymerization-induced alterations in the amphiphile headgroup region.[14] Although a different structure from the parent self-assembled template is produced after UV-irradiation, this reconstructive morphosynthesis does yield a well-ordered, mechanically durable nanostructured material.[24]

Thermal Properties. The water content and thermal properties of the polymer were characterized by TGA and DSC (Figure 4). TGA indicates that the material does dehydrate during the polymerization process. Frequently, the water content postpolymerization dropped to ca. 2% (w/w) (Figure 4A). The TGA data show that the polymer is considerably more thermally stable than the self-assembled monomer precursor solution. Specifically, the polymer shows a 164 °C increase (from 244 to 408 °C) in the decomposition onset temperature. Furthermore, the observed single-step decomposition profile suggests complete incorporation and polymerization of the IL monomer and PEGDA. The DSC thermogram collected for the second heating and cooling scans (Figure 4B) are devoid of any first-order phase transitions over the entire experimental range studied (−70 to 150 °C), again confirming complete loss of the monomer and comonomer. A secondary phase transition, T_g, is observed in the heating scan with a midpoint positioned at −23.27 °C and is reversible upon cooling. It is noted that the recorded T_g value is considerably lower than the 18 °C previously determined for poly(1-(8-(acryloyloxy)octyl)-3-methylimidazolium chloride).[15] Tang et al.[25] have shown that the T_g of poly(IL)s is highly dependent on the properties of the anion and the polycationic backbone; hence, the literature-reported T_g values for imidazolium-based poly(IL)s show a wide variation between −75 and 110 °C with lower T_g values attainable for systems featuring longer alkyl chains, due to increased polymer backbone flexibility. This may partly explain the dramatic difference in the T_g observed between the two polyacrylate ILs. Furthermore, the recorded T_g value for the *net*-poly[C_{10}mim$^+$][Acr$^-$]-*co*-PEGDA compares favorably to that reported for the poly(1-decyl-3-vinylimidazolium chloride), −17.3 °C, an IL polymer which possesses the same number of carbons in the alkyl chain.[14] The DSC heating scan reveals the loss of the thermal event at 52 °C observed in the monomer−water mixture, indicating the polymerization has served to stabilize the liquid-crystalline phase.

Solvent Interactions. The swelling behavior of *net*-poly[C_{10}mim$^+$][Acr$^-$]-*co*-PEGDA in a variety of solvents was evaluated volumetrically. The study was carried out by determination of the equilibrium volume swelling ratio (V_f/V_0 at t_f = 24 h) in solvents spanning a wide range of (Hansen) solubility parameters (Figure 5). This solubility parameter (δ) is a three-dimensional parameter dividing the total Hildebrand value into three parts: a dispersion force component, δ_d; a polar component (dipole−dipole), δ_p; and a hydrogen-bonding component, δ_h.[15] Previously it has been shown that the swelling ratio will reach a maximum when the solubility parameter of the polymer (δ) matches that of the solvent.[26] As shown in Figure 5, the *net*-poly[C_{10}mim$^+$][Acr$^-$]-*co*-PEGDA did not exhibit significant swelling in any of the solvents studied, with swelling ratios, V_f/V_0, ranging only from 0 to 1.6. Similar studies carried out on poly(1-(8-(acryloyloxy)octyl)-3-methylimidazolium chloride) found swelling ratios that ranged from 0 to 230.[15] The comparatively low swelling observed here for the copolymer suggests a high degree of cross-linking.[27] Maximum swelling of the copolymer was observed in chloroform, with a δ value of 19 $MPa^{1/2}$. This provides an estimation of the solubility parameter for the copolymer and indicates that the copolymer is less polar than that determined for poly(1-(8-(acryloyloxy)octyl)-3-methylimidazolium chloride, where maximum swelling was observed to occur in highly polar solvents such as water and ethanol. The lower polarity for *net*-poly[C_{10}mim$^+$][Acr$^-$]-*co*-PEGDA is attributed to the high cross-link density and thus increased hydrophobicity within the headgroup region of the segregated structure. The solubility characteristics for *net*-poly[C_{10}mim$^+$][Acr$^-$]-*co*-PEGDA compare favorably with that determined for poly(alkyl)acrylates, which show miscibility with weakly polar solvents and are typically in the range of 16−25 $MPa^{1/2}$.[28]

To determine whether the *net*-poly[C_{10}mim$^+$][Acr$^-$]-*co*-PEGDA is a cross-linked copolymer formed from the acrylate anion of the IL and the difunctionalized PEG (PEGDA), we examined the product formed by self-assembly and UV irradiation of the nonpolymerizable form of the IL (i.e., [C_{10}Mim$^+$][Cl$^-$]) with PEGDA. The self-assembled mixture of this ionic liquid in 12 ± 2% (w/w) water with the comonomer (PEGDA) and the photoinitiator (Darcour 1173) was studied using polarized optical microscopy (Figure 6A). The prepolymerized composition is not

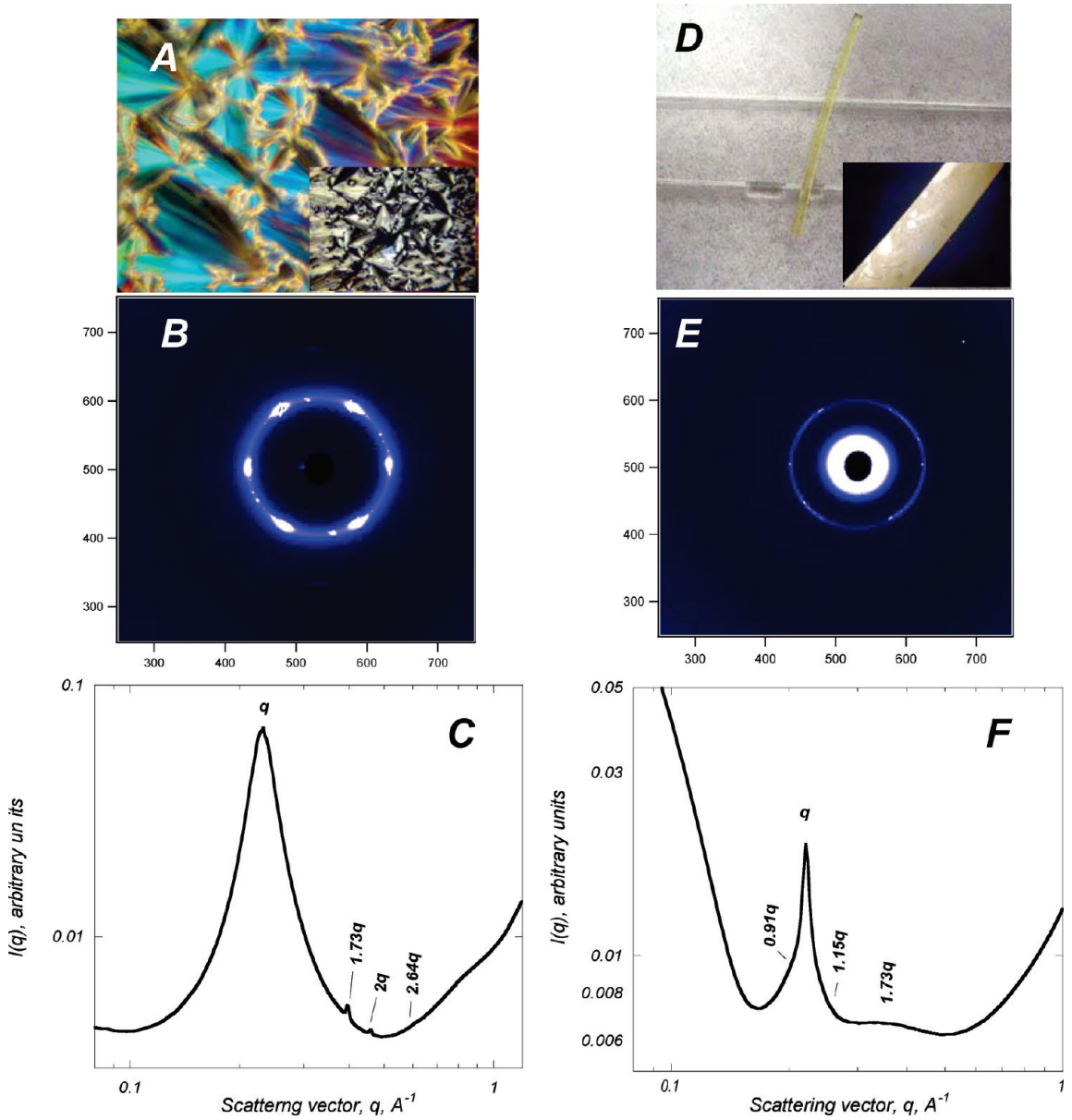

Figure 2. (A) Representative polarized optical micrographs, (B) 2-D small-angle X-ray scattering pattern, and corresponding (C) azimuthally averaged SAXS data collected on mixture of $[C_{10}mim^+][Acr^-]$, $\Phi_{monomer} = 0.879$; water, $\Phi_{water} = 0.111$; PEGDA, $\Phi_{comonomer} = 0.008\,63$; Darocur 1173, $\Phi_{photoini} = 0.001\,72$ before UV irradiation. (D) Digitial photograph (inset, shows sample when viewed under polarized optical light), (E) 2-D SAXS pattern, and (F) azimuthally averaged SAXS curve obtained after UV-irradiation of quaternary mixture for 30 min.

optically birefringent at room temperature but, when cooled to 4 °C, shows focal conic textures under polarized light (Figure 6A, inset). The lack of any observed optical birefringence could be indicative of either an isotropic phase or one that possess cubic symmetry.[29,30] The appearance of focal conic textures upon cooling to 4 °C is consistent with the observed small endothermic transition at 8.7 °C in the DSC heating scan (data not shown).

The SAXS data collected on the mixture prior to UV irradiation at 25 °C are presented in Figure 6B,C. The 2-D image shows a 10-spot pattern characteristic of a bicontinuous cubic structure (Figure 6B). Bicontinuous cubic structures are made up of interpenetrating networks of two phases (e.g., aqueous and organic components). The integrated data (Figure 6C) show two prominent reflections positioned at $q = 0.222$ and 0.259 Å^{-1}. The ratio of these two peaks, q_2/q_1, is 1.16, which may suggest the presences of a double-gyroid structure. The double-gyroid mesophase structure, which consists of two interpenetrating networks formed by 3-fold connectors, is known to occur in many lyotropic and thermotropic liquid crystals derived from block copolymers or lipids.[31,32] The lack of well-resolved reflections at higher q does not permit accurate determination of the bicontinuous cubic space group.[29] Bicontinuous structures have been reported in other self-assembled ionic liquid−water binary mixtures, having specifically been observed as intermediate phases transitioning between lamellar → hexagonal → discrete cubic phases.[16,30,33]

Photopolymerization of the $[C_{10}mim^+][Cl^-]$, PEGDA-based composition produced a transparent, self-supporting glass-like material that has nearly an identical appearance to the network copolymer (Figure 6D). Under polarized light, the polymerized product was highly birefringent, suggesting a liquid crystalline material (Figure 6D, inset). The structure was more fully determined by SAXS. The 2-D pattern (as shown in Figure 6E) possesses textures with 4-fold symmetry. It is noted that the diffraction arcs on the meridian are stronger in intensity than the equatorial ones.

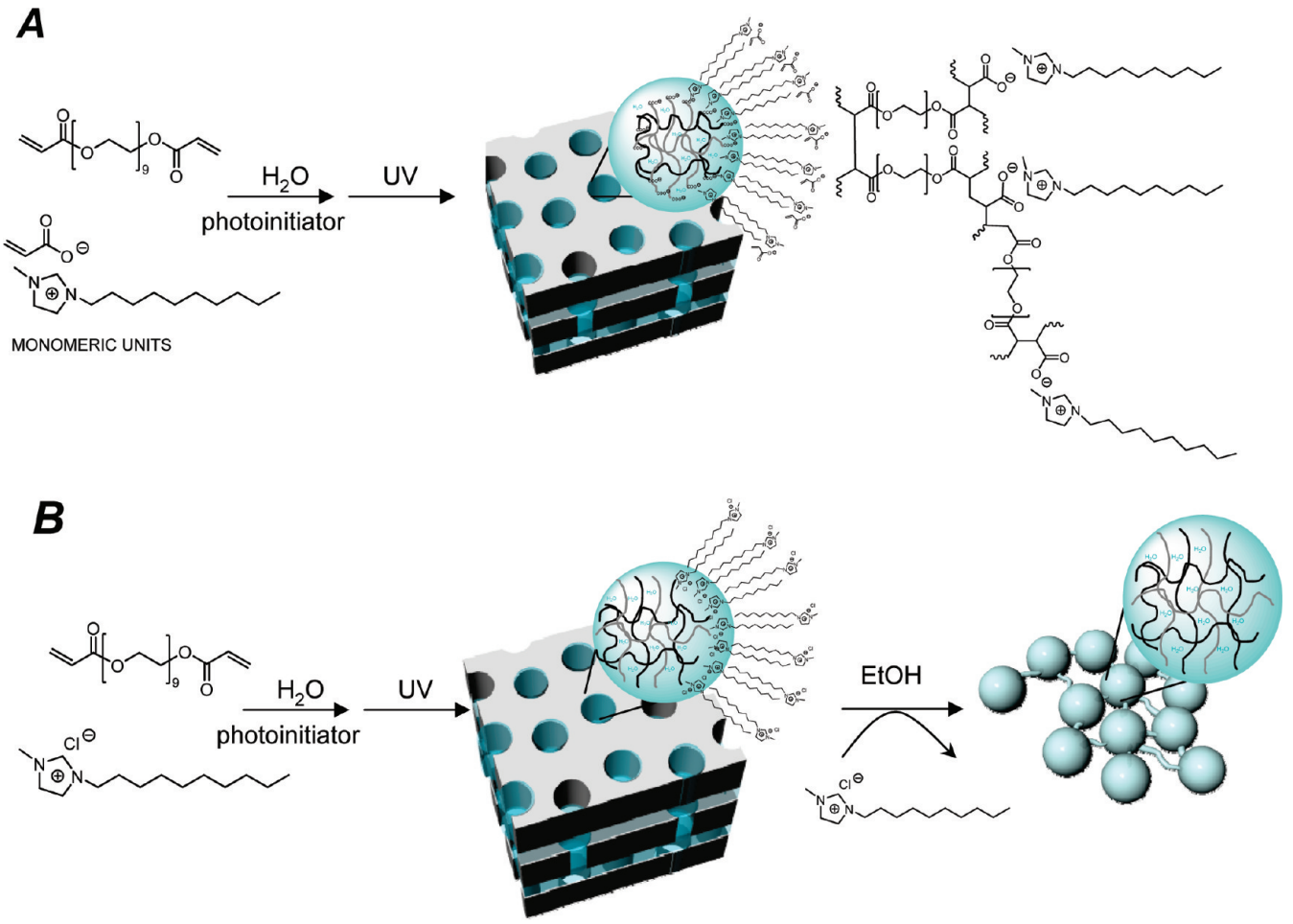

Figure 3. Schematic illustrations of proposed structure for the (A) *net*-poly[$C_{10}mim^+$][Acr^-]-*co*-PEGDA and (B) 1-decyl-3-methylimidazolium chloride, [$C_{10}mim^+$][Cl^-], encapsulated in *net*-PEGDA composite.

The azimuthally averaged data (Figure 6F) show Bragg peaks at 0.9q, q, 1.15q, and $\sqrt{3}$ (q = 0.19, 0.22, 0.25, and 0.38 $Å^{-1}$), consistent with a HPL phase very similar to that determined for the network copolymer (Figure 3B).[34] The position of the first-order peak yields a d-spacing of 28.5 Å. Here, considerably less diffuse low-q scattering and a significantly sharper $\sqrt{3}$ peak are noted compared to that observed for *net*-poly[$C_{10}mim^+$][Acr^-]-*co*-PEGDA, indicating that the material formed here adopts a HPL structure where the in-plane pores have formed into a close-packed hexagonal array.

The material is also found to dehydrate during the polymerization process, with the water content of the postpolymerized material dropping to 5% (w/w) (Figure 4C). In addition to the water loss, the thermogram shows two additional degradation steps at 256 and 405 °C. The derivative thermogravimetric (DTG) curves of the [$C_{10}mim^+$][Cl^-]/PEGDA-based composition (Figure 4C) show a weight loss of 11 wt % at 256 °C, which is attributed to the [$C_{10}mim^+$][Cl^-] (Supporting Information Figure S4). The second weight loss step, at 405 °C, comprises a significant fraction, 77 wt %, and is assigned to the polymerized PEGDA (Supporting Information Figure S3). Thus, comparison of the degradation profiles collected on the two polymerized materials confirms incomplete incorporation of the nonpolymerizable ionic liquid, [$C_{10}mim^+$][Cl^-]. This observation was expected considering the IL lacks moieties appropriate for its covalent integration or copolymerization. Thus, the DTG curve suggests that the material is a network homopolymer of PEGDA that has encapsulated the self-organized IL. The [$C_{10}mim^+$][Cl^-]-PEGDA-based materials shows a very similar DSC scan to that recorded on the *net*-poly[$C_{10}mim^+$][Acr^-]-*co*-PEGDA copolymer (Figure 4D). Here, too, the second heating and cooling scans are devoid of any first-order phase transitions over the experimental range studied but contain a secondary phase transition, T_g, with a midpoint positioned at −26.97 °C (heating scan). This transition is reversible upon cooling. The T_g for this material is only slightly reduced compared to that recorded for the copolymer, which could be attributed to a minor reduction in cross-linking. Prior studies of cross-linked PVA, for example, have shown that the T_g increases slightly as the extent of cross-linking increases.[35]

Additional confirmation that the [$C_{10}mim^+$][Cl^-] is physically trapped rather than covalently integrated within the *net*-PEGDA matrix was obtained by evaluating the product after extensive washing (Soxhlet) of a sample with ethanol. ^{1}H NMR spectroscopy of the extract revealed significant loss of the nonpolymerizable, [$C_{10}mim^+$][Cl^-], with only 22 ± 10% being retained in the polymer matrix. This is in contrast to that determined for the system employing [$C_{10}mim^+$][Acr^-], where 93% was retained, clearly confirming the noncovalent integration of [$C_{10}mim^+$][Cl^-].

The structure of the [$C_{10}mim^+$][Cl^-]-extracted solid polymer was examined by SAXS (Figure 7A). After washing with ethanol, the polymer becomes opaque and shows a scattering pattern devoid of long-range structural ordering on the length scale examined here (10 → 315 Å). That is, the recorded SAXS curve possesses only form factor scattering

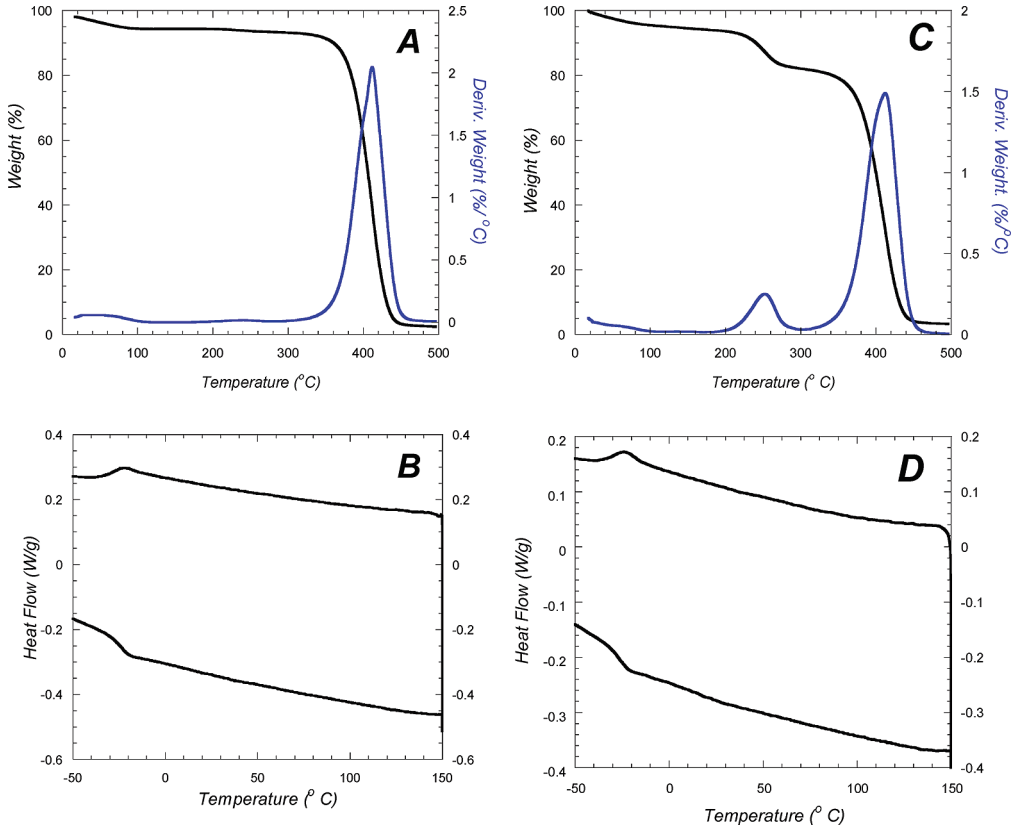

Figure 4. (A) Percentage (black) and derivative weight loss, DTG (blue), curves determined by thermogravimetric analysis (TGA) and (B) DSC for photopolymerized mixture composed of $[C_{10}mim^+][Acr^-]$, $\Phi_{monomer} = 0.790$; water, $\Phi_{water} = 0.117$; PEGDA, $\Phi_{comonomer} = 0.0776$; Darocur 1173, $\Phi_{photoini} = 0.0150$. (C) Percentage (black) and derivative weight loss, DTG (blue), curves determined by thermogravimetric analysis (TGA) and (D) DSC for photopolymerized mixture of composed of $[C_{10}mim^+][Cl^-]$, $\Phi_{IL} = 0.833$; water, $\Phi_{water} = 0.0639$; PEGDA, $\Phi_{comonomer} = 0.0934$; Darocur 1173, $\Phi_{photoini} = 0.001\,80$.

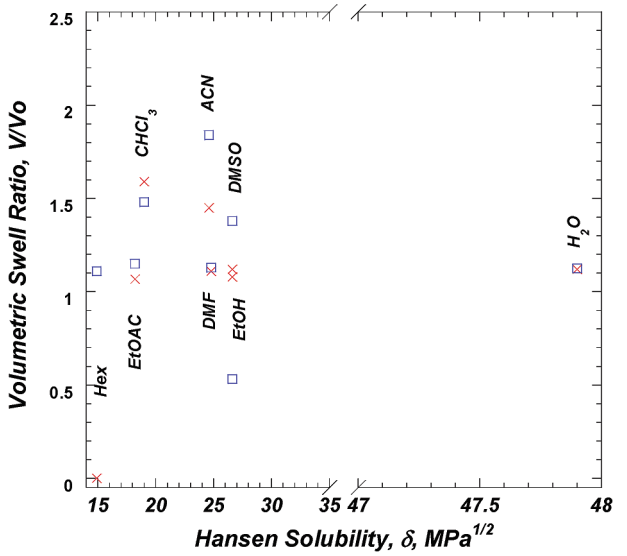

Figure 5. Equilibrium volume changes (V/V_0) of *net*-poly$[C_{10}mim^+][Acr^-]$-*co*-PEGDA (red data points) and 1-decyl-3-methylimidazolium chloride, $[C_{10}mim^+][Cl^-]$, encapsulated in *net*-PEGDA (blue data points) as a function of Hansen solubility parameter evaluated for a range of organic solvents and water after 24 h of incubation.

showing a typical Porod scattering region.[36] Analysis of the Porod region can be carried out by plotting ln I vs ln q.[37] In this region the SAXS intensity follows the expected power-law decay k^{-n} with a gradient of -3.5, suggesting tightly packed polymer chains with sharp interfaces (Figure 7A, inset). The absence of long-range structural order suggests that the self-assembled $[C_{10}mim^+][Cl^-]$ ionic liquid act as a template for the preferential localization and polymerization/cross-linking of the PEGDA within the pore structure of the HPL phase of the self-assembled composite (Figure 3B). Upon solvent extraction of the $[C_{10}mim^+][Cl^-]$ a material composed of dense regions of polymerized PEGDA spheres embedded and cross-linked within an amorphous PEGDA matrix is left (Figure 3B). Thus, since the PEGDA is preferentially solubilized within the ordered aqueous channels of the HPL structure, the hydrophilic pores serve to template the formation of near-spherical cross-linked PEGDA (Figure 3B).

It is noted that a similar SAXS study evaluating the structure after solvent washing/incubation has been initiated for the *net*-poly$[C_{10}mim^+][Acr^-]$-*co*-PEGDA copolymer. These studies found that the copolymer exhibits complex behavior with structural variation depending on the type of solvent and time of exposure to it. For example, after short exposure to ethanol (i.e., days) the structure is preserved but extended incubation (6 months) in ethanol leads to significant reduction and change in the mesophase structure as indicated by the loss of the sharp, well-resolved Bragg reflection at 0.22 $Å^{-1}$ and the appearance of several broad features in the SAXS profile as shown in Figure 7B (dashed line). The SAXS profile collected on samples subjected to extended exposure (6 months) to ethyl acetate, however, show retention of the original ordered mesophase structure (Figure 7B, solid line). The results suggest two possibilities, extraction or ion exchange, by which IL integrity can be altered during prolonged exposure to a solvent. For the *net*-poly$[C_{10}mim^+][Acr^-]$-*co*-PEGDA copolymer cation exchange is expected to occur. Prior work on other polyacrylate anions has demonstrated that the larger the cation the

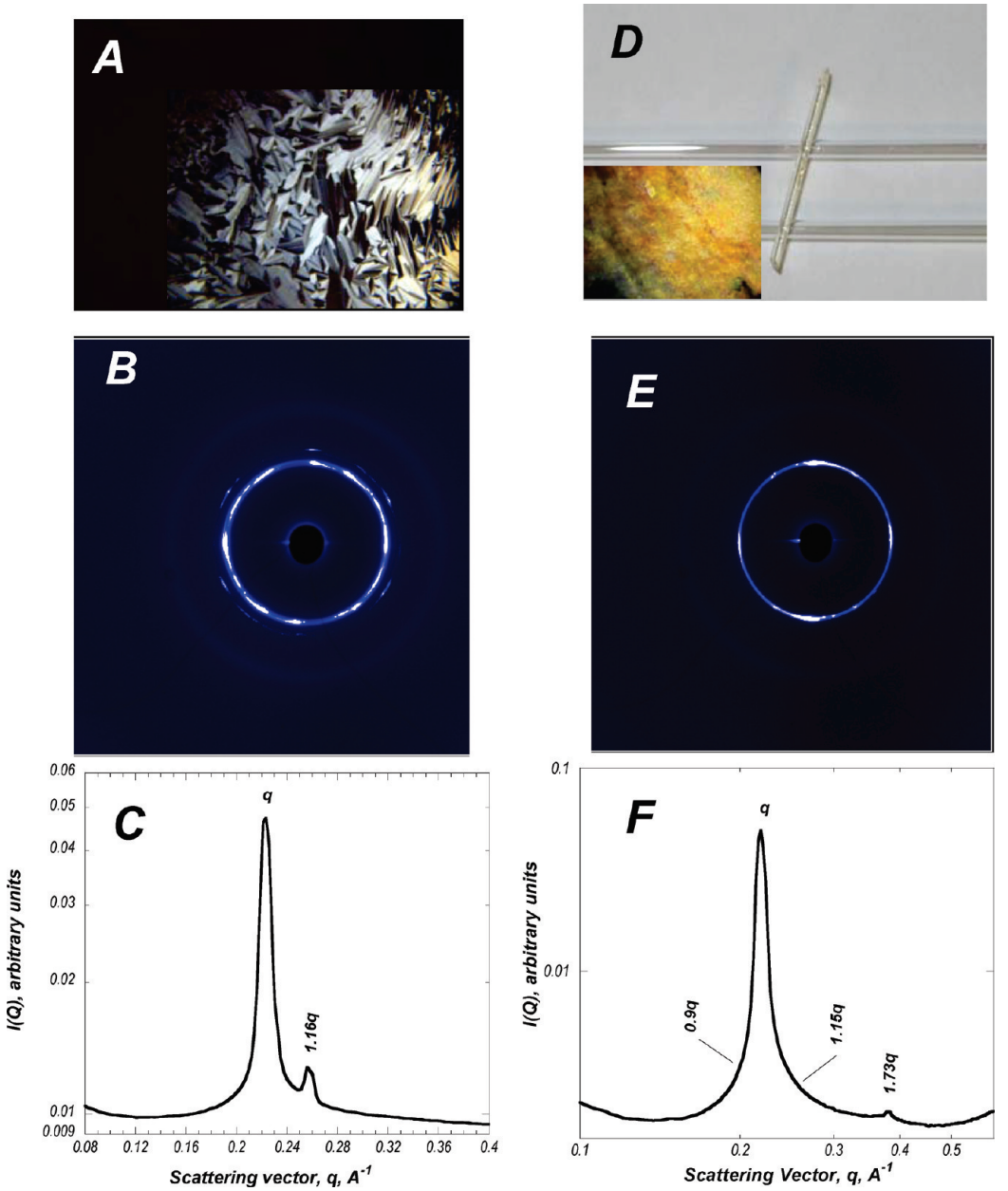

Figure 6. (A) Representative polarized optical micrograph, (B) 2-D small-angle X-ray scattering pattern, and corresponding (C) azimuthally averaged SAXS data collected on a mixture composed of $[C_{10}mim^+][Cl^-]$, $\Phi_{IL} = 0.833$; water, $\Phi_{water} = 0.0639$; PEGDA, $\Phi_{comonomer} = 0.0934$; Darocur 1173, $\Phi_{photoini} = 0.001\,80$ prior to UV irradiation. (D) Digital photograph of photopolymerized product (inset is a polarized optical micrograph), (E) 2-D SAXS pattern, and (F) azimuthally averaged SAXS curve obtained after UV-irradiation of quaternary mixture for 30 min.

more facile the proton exchange.[38] Further studies examining proton exchange of the $[C_{10}mim^+]$ cation from the *net*-poly$[C_{10}mim^+][Acr^-]$-*co*-PEGDA copolymer to produce poly$[H^+][Acr^-]$-*co*-PEDGA will require further examination and will be presented elsewhere.

Finally, the solvent interactions of the $[C_{10}mim^+][Cl^-]$-based material was examined volumetrically employing the same solvents as those used for *net*-poly$[C_{10}mim^+][Acr^-]$-*co*-PEGDA copolymer. As shown in Figure 5, the solubility characteristics determined for the $[C_{10}mim^+][Cl^-]$-derived system are very similar to that found for the *net*-poly $[C_{10}mim^+][Acr^-]$-*co*-PEGDA copolymer. That is, the polymer did not dilate significantly with swelling ratios ranging from 0.5 to 1.8 (hexane to acetonitrile). Maximum swellability was observed upon incubation in acetonitrile, a more polar solvent than chloroform, which yielded the largest volume ratio change for the *net*-poly$[C_{10}mim^+][Acr^-]$-*co*-PEGDA copolymer. Network polymer swelling/solubility characteristics are known to be a complicated property depending on polymer architecture, degree of cross-linking, and chemical composition.[39] Here, the observed increased swelling in a more polar solvent most likely arises from changes in the degree of cross-linking and chemical composition (i.e., the nature of the formed polymer network) since SAXS studies demonstrated no changes in architecture between the two materials. Changes in chemical composition are, however, expected between the two systems. That is, during the course of the solvent swelling studies (24 h) loss of the $[C_{10}mim^+][Cl^-]$ most likely occurs, leaving primarily a PEGDA homopolymer. A PEGDA homopolymer would be expected to be more hydrophilic than a material containing ionic liquid. In addition to these changes in chemical composition, the greater swellability in a more polar solvent may also be attributed to a lower degree of cross-linking.

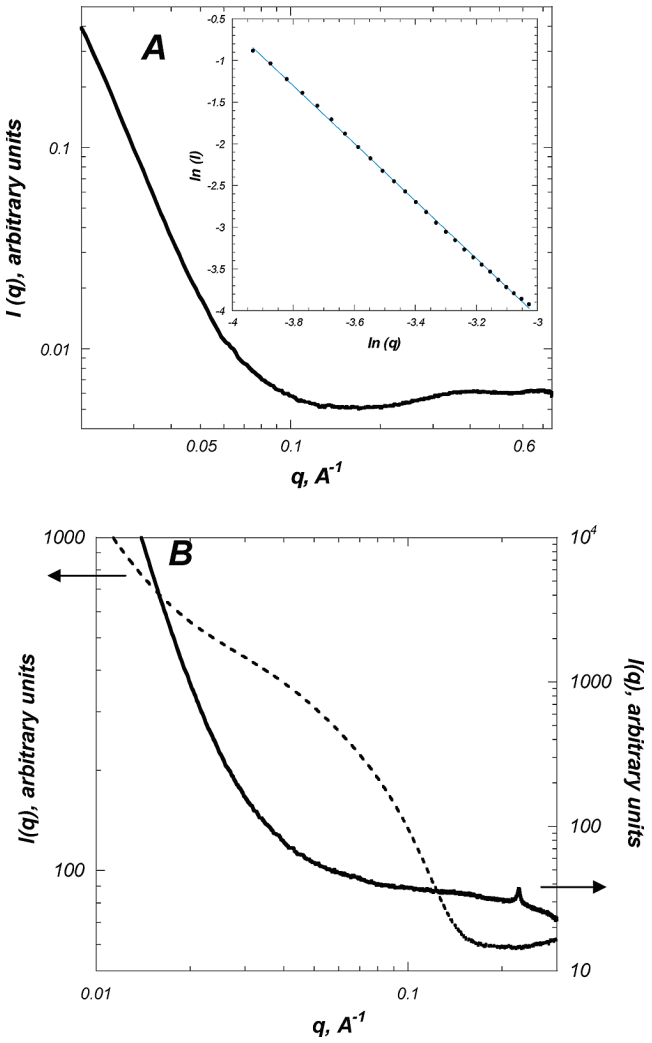

Figure 7. (A) SAXS pattern collected on a $[C_{10}mim^+][Cl^-]$ encapsulated in *net*-PEGDA composite that was subjected to Soxhlet extraction in ethanol for 3 days. Inset shows a logarithmic plot of the scattered X-ray intensity vs q. (B) SAXS pattern collected on *net*-poly$[C_{10}min^+]$-[Acr]-*co*-PEGDA subjected to 6 months of incubation in 190 proof, 95% ethanol (dashed line) and one subjected to 6 months incubation in ethyl acetate (solid line).

Unlike the copolymer, here the noncovalent incorporation of the ionic liquid is expected to yield a reduction in the number of cross-links, which is also confirmed by the slight reduction in the observed T_g.

Conclusions

Polymerization through the counteranion of a self-assembled ionic liquid amphiphile has been demonstrated. Specifically, an IL comprising a decylmethylimidazolium cation paired with a polymerizable (acrylate) anion is shown to self-assemble when dispersed in water. Addition of a difunctional comonomer/cross-linker, PEG diacrylate, and a photoinitiator to the IL monomer−water mixture does not inhibit self-assembly, with SAXS confirming a well-ordered 2-D hexagonal structure. Most likely this is due to the preferential solubility of the PEGDA within the water-rich region of the segregated material, which does not negatively impact the amphiphile organization. UV irradiation of the assembled mixture causes the copolymerization and cross-linking between the electrostatically associated IL anion and the PEGDA within the water phase, yielding a transparent, glassy-like, mechanically durable polymer network. The formed copolymer network adopts a hexagonal perforated lamellar structure, HPL, a mesoscale architecture that is a hybrid between lamellar and 2-D hexagonal. That is, the IL cation assembles into bilayers separated by water channels, a local architecture similar to that observed in a biological membrane. In addition, the amphiphile bilayers possess hydrophilic pores that are organized with hexagonal symmetry. The IL anion and comonomer, PEGDA, within the water phase form a network wrapped around the organized IL cation bilayer (Figure 3A). This permits construction of a model membrane that is anchored to an electrostatically associated polymer matrix, reinforcing the bilayer structure, and hence, it is functioning as a cytoskeleton mimic. The hierarchical structure offers the possibility of sequestering both lipophilic and water-soluble guests into the segregated domains. Moreover, the unperturbed bilayer will allow for the full incorporation of transmembrane proteins. The resultant nanostructured material has been shown to have good thermal stability and is well cross-linked, as suggested by its inability to dissolve or swell in a wide variety of organic solvents or water. Extended incubation in 95% ethanol, however, induced significant changes in the copolymer nanostructure, suggesting the possibility of IL cation exchange. Future studies will examine the stability and integration of both water-soluble and membrane proteins into the network copolymer and the use of the tunable mesophase architecture to regulate the internal packing arrangement of the encapsulated guests. The mimicking of a cytoskeletal arrangement represents an important first step in preparing durable materials that will permit the reconstitution of membrane proteins. Ultimately such studies could lead to the fabrication of assemblies capable of withstanding the challenging environments such as those found in micro- or nanoscale devices.

Acknowledgment. The authors thank Dr. Byeongdu Lee for valuable discussions on the SAXS data and Professor Tom Irving and Dr. Liang Guo for rapid access and use of the BioCAT, SAXS instrument. We also acknowledge Dr. Sungwon Lee for assistance in rendering the POV ray images. This work was performed under the auspices of the Office of Basic Energy Sciences, Division of Materials Sciences, United States Department of Energy, under Contract DE-AC02-06CH11357.

Supporting Information Available: ^1H and ^{13}C spectra of 1-decyl-3 methylimidazolium acrylate; thermograms of $[C_{10}mim^+][Cl^-]$ and polymerized PEGDA. This material is available free of charge via the Internet at http://pubs.acs.org.

References and Notes

(1) LeDuc, P. R.; Bellin, R. M. *Ann. Biomed. Eng*. **2006**, *34*, 102–113.
(2) Tanaka, M.; Rossetti, F.; Kaufmann, S. *Biointerphases* **2008**, *3*, FA12–FA16.
(3) Ge, L. Q.; Mohwald, H.; Li, J. B. *Colloids Surf., A* **2003**, *221*, 49–53.
(4) Antunes, F. E.; Marques, E. F.; Miguel, M. G.; Lindman, B. *Adv. Colloid Interface Sci*. **2009**, *147−148*, 18–35.
(5) Germain, M.; Grube, S.; Carriere, V.; Richard-Foy, H.; Winterhalter, M.; Fournier, D. *Adv. Mater*. **2006**, *18*, 2868–2871.
(6) Meier, W.; Hotz, J.; Gunther-Ausborn, S. *Langmuir* **1996**, *12*, 5028–5032.
(7) Zhu, C.; Lee, J.-H.; Raghavan, S. R.; Payne, G. F. *Langmuir* **2006**, *22*, 2951–2955.
(8) Stauch, O.; Schubert, R.; Savin, G.; Burchard, W. *Biomacromolecules* **2002**, *3*, 565–578.
(9) Meier, W. *Chem. Rev*. **2000**, *29*, 295–303.
(10) Mueller, A.; O'Brien, D. F. *Chem. Rev*. **2002**, *102*, 727–757.
(11) Hotz, J.; Meier, W. *Surfactant Sci. Ser*. **2001**, 501–514.
(12) Hotz, J.; Meier, W. *Langmuir* **1998**, *14*, 1031–1036.
(13) Gutmayer, D.; Thomann, R.; Bakowsky, U.; Schubert, R. *Biomacromolecules* **2006**, *7*, 1422–1428.
(14) Batra, D.; Seifert, S.; Varela, L. M.; Liu, A. C. Y.; Firestone, M. A. *Adv. Funct. Mater*. **2007**, *17*, 1279–1287.

(15) Batra, D.; Hay, D. N. T.; Firestone, M. A. *Chem. Mater*. **2007**, *19*, 4423–4431.
(16) Batra, D.; Seifert, S.; Firestone, M. A. *Macromol. Chem. Phys*. **2007**, *208*, 1416–1427.
(17) Vanderhooft, J. L.; Mann, B. K.; Prestwich, G. D. *Biomacromolecules* **2007**, *8*, 2883–2889.
(18) Clapper, J. D.; Guymon, C. A. *Macromolecules* **2007**, *40*, 1101–1107.
(19) MacDonald, R. T.; Pulapura, S. K.; Svirkin, Y. Y.; Gross, R. A.; Kaplan, D. L.; Akkara, J.; Swift, G. S. W. *Macromolecules* **1995**, *28*, 73–78.
(20) Greaves, T. **2006**, *100*, 22479−22487.
(21) Malhotra, S.; Zhao, H. *Phys. Chem. Liq*. **2003**, *41*, 545–557.
(22) Firestone, M. A.; Dietz, M. L.; Seifert, S.; Trasobares, S.; Miller, D. J.; Zaluzec, N. J. *Small* **2005**, *1*, 754–760.
(23) Hamley, I. W.; Castelletto, V.; Mykhaylyk, O. O.; Yang, Z.; May, R. P.; Lyakhova, K. S.; Sevink, G. J. A.; Zvelindovsky, A. V. *Langmuir* **2004**, *20*, 10785–10790.
(24) Hentze, H. P.; Kaler, E. W. *Chem. Mater*. **2003**, *15*, 708–713.
(25) Tang, J. B.; Tang, H. D.; Sun, W. L.; Radosz, M.; Shen, Y. Q. *J. Polym. Sci., Part A: Polym. Chem*. **2005**, *43*, 5477–5489.
(26) Liao, D. C.; Chern, Y. C.; Han, J. L.; Hsieh, K. H. *J. Polym. Sci., Part B: Polym. Phys*. **1997**, *35*, 1747–1755.
(27) Bryant, S. J.; Davis-Arehart, K. A.; Luo, N.; Shoemaker, R. K.; Arthur, J. A.; Anseth, K. A. *Macromolecules* **2004**, *37*, 6726–6733.
(28) *Polymer Handbook*, 3rd ed.; Grulke, E. A., Ed.; Wiley-Interscience: New York, 1989.
(29) Avgeropoulos, A.; Dair, B. J.; Hadjichristidis, N.; Thomas, E. L. *Macromolecules* **1997**, *30*, 5634–5642.
(30) Zhao, Y.; Chen, X.; Wang, X. *J. Phys. Chem. B* **2009**, *113*, 2024–2030.
(31) Jung, M.; German, A. L.; Fischer, H. R. *Colloid Polym. Sci*. **2001**, 105–111.
(32) Sun, R. G.; Zhang, J. *J. Phys. D: Appl. Phys*. **2004**, *37*, 463–467.
(33) Strom, P.; Anderson, D. M. *Langmuir* **1992**, *8*, 691–709.
(34) Zhu, L.; Cheng, S. Z. D.; Huang, P.; Ge, Q.; Quirk, R. P.; Thomas, E. L.; Lotz, B.; Hsiao, B. S.; Yeh, F.; Liu, L. Z. *Adv. Mater*. **2002**, *14*, 31–34.
(35) Ruiz, J.; Mantecon, A.; Cadiz, V. *Polymer* **2001**, *42*, 6347–6354.
(36) *Small Angle X-ray Scattering*; Porod, G., Ed.; Academic Press: London, 1982.
(37) Hasegawa, H.; Hashimoto, T.; Kawai, H.; Lodge, T. P.; Amis, E. J.; Glinka, C. J.; Han, C. C. *Macromolecules* **1985**, *18*, 67–78.
(38) DeStefano, C.; Gianguzza, A.; Piazzese, D.; Sammartano, S. *J. Chem. Eng. Data* **2000**, *45*, 876–881.
(39) Finne, A.; Albertsson, A.-C. *J. Polym. Sci., Part A: Polym. Chem*. **2003**, *41*, 1296–1305.